IMPACT OF CHOKE MANAGEMENT ON THE RETURN ON INVESTMENT IN THE VACA MUERTA RESERVOIR

Ariel Sánchez Camus[1,2], Ricardo Ramos[1,3,4], Nicolás Polimeni[4]

1: Tections S.A. acamus@tections.com.ar, rramos@tections.com.ar

2: Facultad de Ciencias Astronómicas y Geofísicas (UNLP)

3: Facultad de Ingeniería (UNLP)

4: Solaer Ingeniería S.A. npolimeni@solaeringenieria.com

Palabras clave: manejo de choke, Vaca Muerta, producción, geomecánica, simulación FEM, inversión

RESUMEN

Las mudrocks orgánicas son reservorios dinámicos cuyas propiedades petrofísicas y mecánicas varían con el soterramiento en el largo plazo (tiempo geológico) y con la producción en el corto plazo (semanas, meses, años). En condiciones de reservorio, la producción de hidrocarburos va a estar gobernada por fuerzas de presión, el campo de esfuerzos y por la conectividad hidráulica (interna o externa) que pudieran propiciarles las fracturas naturales o las inducidas por fracturamiento hidráulico. La política de manejo del choke es crucial para regular el flujo de hidrocarburos tanto en la etapa inicial de flowback como durante el período de producción del pozo. Contar con un modelo geomecánico poroelástico 3-D de elementos finitos (FEM) que permita determinar el tamaño óptimo del choke posibilita seleccionar la mejor estrategia de producción a lo largo de toda la vida útil del pozo. El presente trabajo muestra, mediante simulación numérica, el alto impacto que tiene el manejo de la presión de fondo en la recuperación de hidrocarburos y en la ralentización de la pérdida de permeabilidad de un pozo vertical en la formación Vaca Muerta, ubicado en la ventana de generación de petróleo.

INTRODUCCIÓN

Hydrocarbon production in organic-rich mudrocks is affected by multiple and diverse causes. Among them are the mineralogical, petrophysical and geomechanical characteristics of the reservoir rock (Loucks *et al.* 2012; Loucks and Reed 2014; Sánchez Camus *et al.* 2021), kerogen type, maturity and volume (Lewan and Henry 1999; Lewan 1985; Lewan and Ruble 2002; Lewan and Birdwell 2013), wettability (Bryndzia and Braunsdorf 2014; Jagadisan and Heidari 2019), matrix and organic matter sorption properties (Ross and Bustin 2009; Gasparik *et al.* 2014; Zoback and Kohli 2019), well design, fracture plan and selected completion strategy (Zee Ma and Holditch 2016; Belyadi *et al.* 2019; Zoback and Kohli 2019). Nevertheless, being these reservoirs with dual porosity and at the same time governed by pressure forces, it is exactly the variation of forementioned pressure forces which have the main influence on the reservoir permeability for most of the production (Apaydin *et al.* 2012, Wan *et al.* 2013; Zoback and Kohli 2019). Therefore, choke management policy is crucial for hydrocarbon flow control and the delay of the subsequent compaction and destruction of permeability it causes on the wellbore.

The determination of optimal choke size is not an easy task. If pressure drawdown is too aggressive, production will improve at the beginning; however, this causes a sudden increase in effective stresses which leads to a quick closure of the interconnected fracture system (natural or induced) along with other adverse effects such as proppant embedding or crushing and spalling. On the other hand, a too conservative approach helps preserve the fracture system conductivity, but the production rate increases slowly in the initial stage (Karantinos 2019; Almasoodi *et al.* 2020; Bagci and Stolyarov 2019; Zhao *et al.* 2021). In both cases, the system of microfractures and macrofractures near the wellbore will eventually collapse, leaving a remaining permeability or remaining hydraulic conductivity that will depend on the proppant type, size, mesh, volume and distribution in the fracture system (Hegazy 2016; Irirarte *et al.* 2018; Hryb 2018) and on the matrix and organic matter sorption properties (especially in the gas window). Additionally, in the oil and condensate generation window, pressure and temperature changes may lead to wax and asphaltene precipitation in the reservoir walls, which will decrease even more the rock permeability in the latter production stages.

In general terms, production rates of unconventional wells decrease quickly during the first 2 or 3 years of production. Therefore, it is important to apply a choke management policy that considers the phenomena affecting reservoir permeability, maximizes hydrocarbon recovery and allows a faster return on investment.

The present work shows, by means of numerical simulation (FEM), three pressure management scenarios in a vertical well in the Vaca Muerta formation (VMF), located in the oil generation window. Initially, the FEM poroelastic model is adjusted with the well's production curve and wellhead pressures (history matching). Then, two different scenarios are simulated (considering wellhead pressure 20% above and below history matching pressure), in which the high impact that bottomhole pressure management has on hydrocarbon recovery and reservoir integrity is clear.

PRODUCTION MECHANISMS AND LOCAL COMPACTION

From a petrophysical point of view, matrix porosity of organic-rich mudrocks is composed of four types of porosities classified according to its occurrence and origin. The pore space related to the mineralogical skeleton is classified as intergranular (pores found between particles and crystals) and intragranular (pores located within particles), the space generated inside the particles of kerogen as it cracks to bitumen, oil or gas is known as 'organoporosity' (Loucks *et al.* 2012; Loucks and Reed 2014; Hernández Bilbao 2016), and the space created when microfractures crosscut kerogen and grains is defined as microfracture porosity (Vernik 1994; Al Duhailan *et al.* 2013, 2015; Lewan and Roy 2011; Lewan and Birdwell 2013). The microfracture network is similar to a conventional fracture network in shape but not in scale. It shows some of the fracture characteristics, such as low porosity, high permeability and stress sensitivity. However, its size is on the pore scale (micro-to-nano-scale pore size) and therefore it also shows some characteristics of a low permeability matrix, such as boundary layer effect, threshold pressure gradient, etc.

Saif *et al.* (2017) conducted pyrolysis experiments on Green River Formation samples, going from the oil to the dry gas window. Results showed that higher porosity values corresponded with the most organic-rich zones which, at the same time, were the zones with the highest amount of generated horizontal microfractures. Given the fact that microfractures develop within the matrix, their distribution will affect fluid behavior inside it. Nelson (2009) shows that, in mudrocks, pore size is one or two orders of magnitude above the radius of the smallest hydrocarbon molecule (methane). For this reason, in the oil generation window, liquid hydrocarbon migration inside the matrix will be mainly controlled by the microfracture systems.

Data reported regarding to mudrock matrix permeability shows significant permeability anisotropy (Ghanizadeh *et al.* 2013, Bhandari *et al.* 2015; Pan *et al.* 2015). The ratio of horizontal to vertical permeabilities, kh/kv ranges between 3 to 40 over a wide range of permeability values (100 μD–0.1 nD). Hence, within the reservoir the fluid internal migration occurs mainly in the horizontal direction. Mokhtarin *et al.* (2015) studied permeability anisotropy in outcrop samples of the Mancos formation (Colorado, USA). They found that a sample with a single microfracture showed a permeability one order of magnitude higher than the other twin samples did. Thus, it is to be expected that under reservoir conditions, hydrocarbon filled bed-parallel microfractures increase horizontal matrix permeability by some orders of magnitude (Lewan and Roy 2011; Lewan and Birdwell 2013; Saif *et al.* 2017).

Apaydin *et al.* (2012) studied by means of an analytical model the effect of discontinuous microfractures in a very low permeability rock matrix traversed by macrofractures (induced by hydraulic stimulation). Results showed that the contribution of a certain density and orientation of microfractures to matrix flow capacity will depend on the permeability added by the microfracture system and its connectivity with the macrofracture network. This work showed that a contrast of at least five orders of magnitude is required in order to have a considerable contribution of the microfracture system.

It is for all the foregoing reasons that production rates and cumulative production of this type of reservoirs are ruled by a continuous flow (Darcy) that goes from the low permeability matrix towards the natural and induced fracture systems which are much more permeable (Zoback and Kohli 2019).

Regarding local compaction, organic-rich mudrocks are overpressured reservoirs, most of them showing Biot coefficients below 1, which means that pore pressure is less effective for expanding pores than confining pressure is for closing them (Zoback and Kohli, 2019). This clearly shows how important it is to control the variation of effective stress inside the interconnected fracture system during well production. Experiments show that organic-rich mudrock permeability decreases almost exponentially with the increase of effective stress (Mokhtari *et al.* 2013; Heller *et al.* 2014; Zhou *et al.* 2019; Chen *et al.* 2019).

CASE STUDY

The study well is in the Loma Jarillosa Este block, located in the oil generation window of the VMF– embayment region–at about 500 meters from a normal fault, in the fault damage zone. In this area the stress regime is normal faulting and the horizontal stress anisotropy is very low (Garcia *et al.* 2013; Varela *et al.* 2020). In this well, VMF has an average thickness of 100 meters. The mineralogical composition is comprised mainly of calcite, quartz, feldspar, and several clay minerals, with most of the clay being illite, mica and the mixed illite/smectite phase. The upper (UVM) and middle (MVM) sections were classified as argillaceous marlstones and the lower (LVM) section as a siliceous marlstone. The kerogen content rises from top to base, being the mean volume in the well of 9% for UVM, 13% for MVM and 21% for LVM.

The C33, the C44 and the C55 stiffness parameters of the VTI elastic tensor were calculated using dipole and cross-dipole sonic tools, while the C12 and the C13 were adjusted with the constants taken from core measurements (core extracted from Lower Vaca Muerta). For the purpose of making a seismic interpretation of the permeable fractured zones, it is necessary for the C66 parameter to be obtained from an independent measurement and not as a linear combination of the C44 parameter. The C66 was calculated using the Stoneley wave together with the drilling profiles (Chi and Tang 2006; Sinha *et al.* 2006a).

The formation was divided into 17 anisofacies interpreted for using in the 3D numerical geomechanical model. The anisofacies were calculated as effective mediums; however, in the numerical model the pore pressure and the stress field vary point to point with the depth within each anisofacie. It is assumed that there is no hydraulic connection between anisofacies, or that it is very low if there is any. The orthorhombic elastic tensor in anisofacies with a strong presence of open vertical fractures was estimated applying the model given by Sánchez Camus *et al.* 2018. For further details on the interpretation and characterization carried out in this well, see Sánchez Camus *et al.* 2021.

Pore Pressure and stress field

Organic-rich mudrocks are anisotropic, viscoelastic, porous, overpressured and low permeability media. The rock behaves as closed or open systems depending on the hydraulic connectivity provided by the natural fractures or those induced by hydraulic fracturing. Under reservoir conditions, the pore pressure and the quantity of hydrocarbons in situ will depend on the kerogen chemical composition, its thermal maturity and its volume. The composition will define the hydrocarbons generation time and the types of products to be obtained, while the volume will determine the fluids expansion and the quantity of hydrocarbons generated (Lewan 1985; Lewan and Ruble 2002; Vandenbroucke and Largeau 2007).

Because of the high hydrogen-rich organic matter content, the pore pressure (Pp) in the VMF already reached the minimum horizontal stress (dynamic balance) practically throughout the hydrocarbon generation window. This is the reason why the Pp curve follows a linear trend. If the rock had vertical hydraulic connectivity from top to base, it would also follow a linear trend as a result of pressure equilibrium. In the VMF case, natural fracture systems appear not to contribute significantly to formation permeability. Ukar *et al.* (2020), concluded that in the subsurface, the VMF contains abundant bed-parallel and bed-perpendicular veins of fibrous calcite, completely or partly calcite-filled. Hence, at reservoir conditions the natural fractures systems may not provide fluid flow pathways. Additionally, the thickest and largest bed-parallel veins of fibrous calcite act as seals for the vertical fluid migration (Rodrigues *et al.* 2009; Sosa Massaro 2018). This is the reason why the VMF needs to be hydraulically stimulated to be economically profitable.

The study well is in the fault damage zone of a normal fault system. Fault systems are zones where external hydrocarbon migration is favored, and it will be different for each formation layer. The leak-off gradient will depend on Pp, mineralogy, organic matter content, thermal maturity, type of fluid, wettability, permeability anisotropy, sorption phenomena, mineral diagenesis phenomena, fault plain connectivity, etc. Due to this, and since each organofacie will experiment secondary hydrocarbon migration in a differential way, and most organofacies are not hydraulically connected, the Pp curve is not expected to follow a linear trend in the whole column when near a fault.

Estimating the stress field by using the anisotropic poroelastic equation is not a simple job. Being this a constitutive equation, Biot coefficients and strain field must be calculated for each point (Fjaer *et al.* 2018). In this equation, stresses and strain are two sides of the same coin; to establish a strain field means to establish a stress field and vice versa. Biot coefficients are also very difficult parameters to calculate in reservoir conditions (even in the laboratory). These depend on mineralogy, mechanical anisotropy, effective stress and, to a great extent, on dual porosity (Ma and Zoback 2017; Zoback and Kohli 2019)

With the aim of obtaining a stress field with actual physical sense, i.e. that represents a real equilibrium condition, an algorithm which approximates the stress field and Biot constants point by point was developed. Further details on Pore Pressure and horizontal stress calculation may be found in the Appendix.

FEM NUMERICAL MODEL

A 3-D FEM geomechanical model is built with the objective of studying how the reservoir varies from an initial geostatic state to a final dynamic state of production. This model is poroelastic, which allows finding the equilibrium conditions by coupling the pore pressure changes with the mechanical deformations (Zoback 2007; Fjaer *et al.* 2008). Starting from a mechanical (anisotropic) and petrophysical model, including a stress field characterization, the reservoir conditions are reproduced. Then, the production after completion and hydraulic fracture is simulated.

The flow model in porous media used in the production simulation is fully coupled to the anisotropic poroelastic mechanical model, in such a way that the production modifies not only the pore pressure but also the void ratio, the permeability, and the stress field on the rocky massif, on the well and on the cement shield. The horizontal Darcy permeability of each anisofacie is calibrated with the initial production data together with a vertical permeability consistent with the elastic symmetry of each anisofacie. The fracture permeability is assumed to be isotropic (Apaydin *et al.* 2012) and the rock matrix void ratio is entered from the total porosity log. The initial saturation condition is 100% and a single-phase flow is assumed. It is worth mentioning that the single-phase flow condition may change throughout production. The initial stress field of the production model comes from the fracture model modified by the completion operation (well cementing) (Ramos and Sánchez Camus *et al.* 2017). For additional information regarding this model see Sánchez Camus *et al.* (2021).

Well production simulation results

Figure 1 shows on track 1 the Pp of the reservoir before fracturing, on track 2 the liquid production by layer perforation with a difference in time of 22 days (initial in blue, day 22 in black), and on track 3 the rock elastic symmetry factor. It is observed that, once the vertical hydraulic connectivity is established by induced fracturing, the fluid flows from the layers with

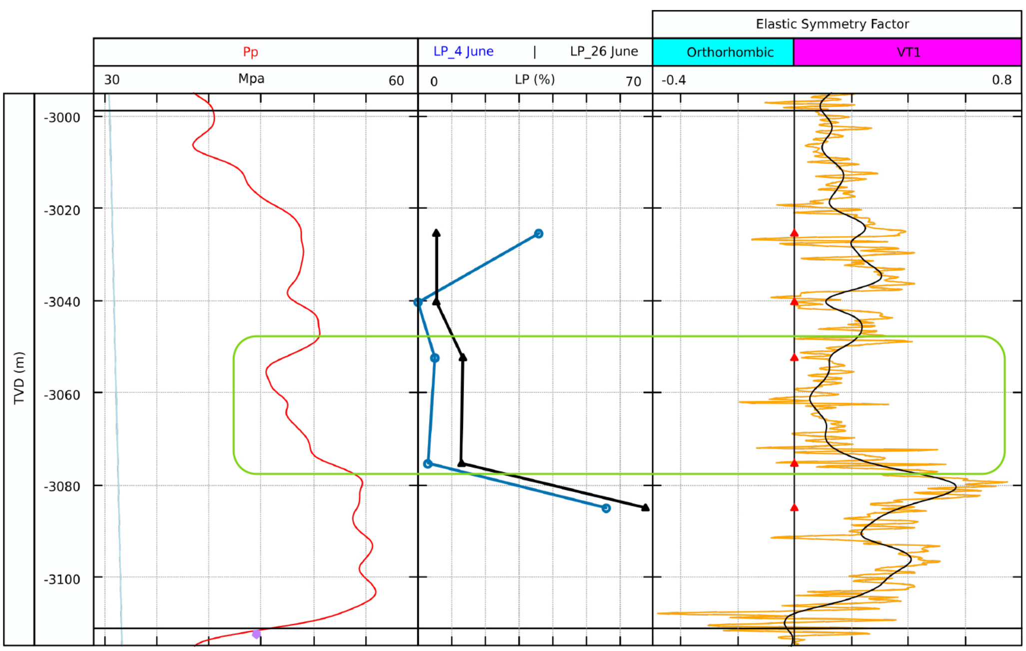

Figure 1. Well tracks.

higher pressure and stronger *in situ* VTI anisotropy to the ones with lower pressure and weaker *in situ* VTI anisotropy. Hence, the low relative pressure and great permeability zones 'will compete for' the hydrocarbon with the areas of higher pressure (and also with the well) once the vertical hydraulic connectivity is established.

The highlighted corridor of Figure 1 had an impact not only on the hydrocarbon production, but also on the well stability and the hydraulic fracturing propagation (Osorio and Musio 2013; Sánchez Camus *et al.* 2021). It would be expected that this zone presents strong *in situ* VTI anisotropy and high pore pressure due to the fabric anisotropy, the high kerogen content and thermal maturity that it exhibits; however, it presents weak *in situ* VTI anisotropy and suffers a pressure drop. This section of the well is a corridor that presents a complex system of open fractures hydraulically connected to the fault. For the sake of simplicity, the anisofacies were characterized with two sets of fractures perpendicular to each other, where the set parallel to the SH presents a higher density of fractures than the set parallel to the fault strike line.

The effect that hydraulic fracture has on the formation is not only the mechanical fracturing generation and its subsequent filling with a proppant agent, but also the modification of the pore pressure field by infiltration in the area close to the fracture. This overpressured zone infiltrated with water is the one that the well will produce first. Consequently, the water percentage in the initial production will be very high, which is verified in the production records of the operator company.

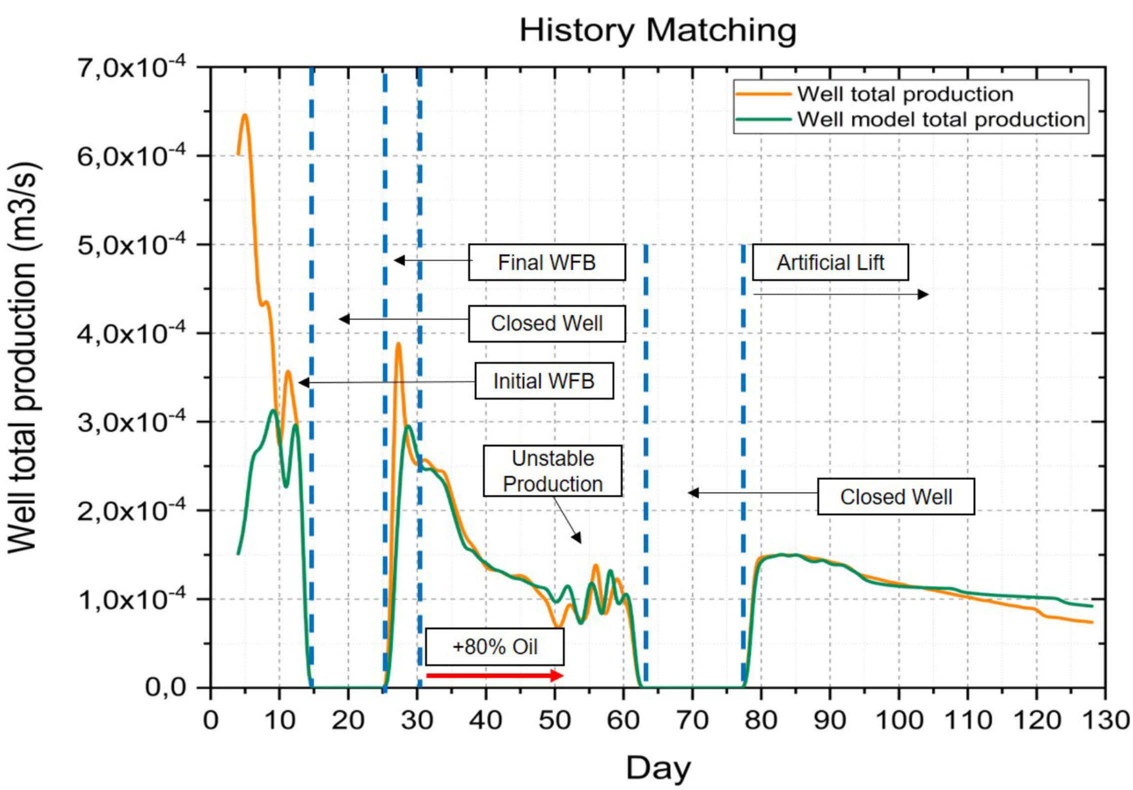

Figure 2. History matching.

Figure 2 shows the well production log for the first 128 days compared to the obtained production model. The discrepancy between the model and the well production log ends at the point where the water flowback (WFB) peaks and the production is mostly oil; this is since the applied pore pressure field is consistent with the pre-fracture reservoir conditions. The point at which oil production exceeds 80% of total liquid is highlighted. After the zone of unstable production, the well was closed, and an electro-submersible pump was installed. Finally, the long-term production is achieved with the pump assistance. See that the artificial lift period between day 80 and day 128 was also reproduced by the model.

As mentioned above, the permeability anisotropy of organic-rich mudrocks is very significant. Effective vertical stress will increase when pore pressure decreases, which will subsequently cause the decrease of the horizontal permeability associated with hydrocarbon filled bed-parallel microfractures and with the least stiff interconnected pores. It is worth mentioning that, in many laboratory studies, increasing effective stress tends to lower permeability more in the vertical than the horizontal direction mainly due to the increased tortuosity of vertical flow pathways (Arch and Maltman 1990; Zoback and Kohli 2019). Therefore, the increase of effective vertical stress will decrease the rock permeability in both directions.

Figure 3 and Figure 4 (centered on the well axis) show the effective vertical stress of two different perforation layers in a line perpendicular to the fracture plane for five specific production days. The increase in this stress near the wellbore is due to the pore pressure drop in the surroundings of the hydraulic fracture. As the permeability is related with the void ratio, higher stresses are correlated with lower permeabilities. If the production gradient is too high, the consequent effective vertical stress will cause a permeability barrier that will decrease hydrocarbon recovery even with a high differential pressure between the well and the far field. The microfracture systems that affect fluid flow, along with the interconnected least stiff pores, will have more possibilities to remain open and be recharged by hydrocarbons if the pore pressure remains as high as possible. The resulting permeability between the well and the far field will also be higher, with a positive impact on the total oil recovery. Note in Figure 4 that the hydrocarbon migration into the fractured corridor caused a decrease of the effective vertical stress away from the surroundings of the hydraulic fracture.

A modification in the production strategy with the purpose of getting a lower rate of compaction around the hydraulic fracture should decrease the mentioned permeability barrier effect. This means that the differential pressure between the well and the far field should be lower. In order to test this hypothesis, the built model was run with a wellhead pressure 20% above and 20% below the history match (20% chosen arbitrarily).

Figure 5 shows the effective vertical stress in the first perforated layer (3025,5 m) on day 34 for the three models described. The model with wellhead pressure 20% above actual field values showed a lower effective vertical stress, as opposed to the model with wellhead pressure 20% below, which showed an increase in effective vertical stress.

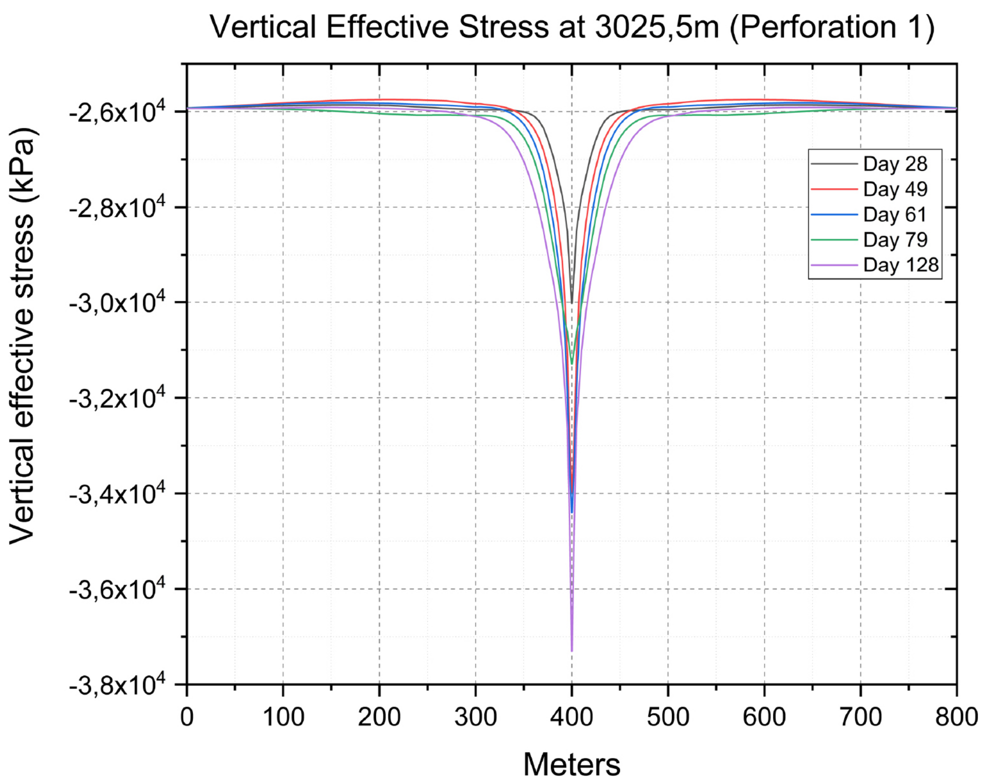

Figure 3. Effective vertical stress at Perforation 1.

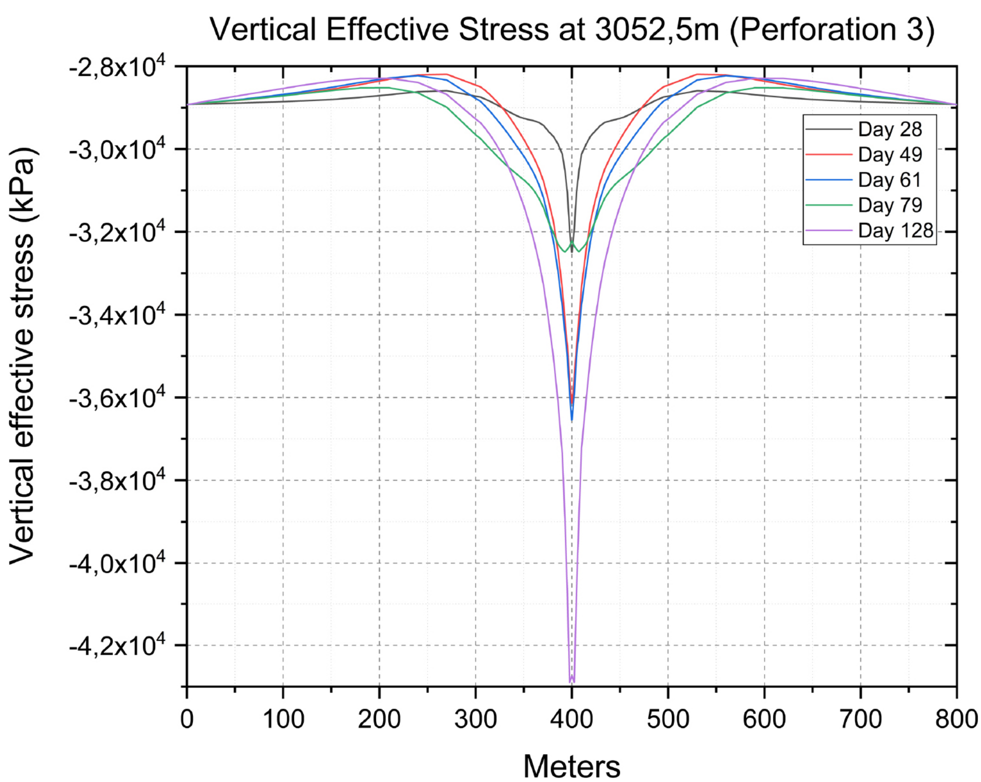

Figure 4. Effective vertical stresses at Perforation 3.

Figure 6 shows the resulting production rate in each of the three scenarios. A higher differential pressure between the well and the far field produces a peak in the flowrate followed by a sudden drop. This drop is due to the mentioned barrier effect. Additional phenomena like proppant crushing and spalling or embedding are not included in this model; considering them could significantly affect modeled cumulative production.

Figure 7 shows the cumulative production curves. The scenario where wellhead pressure was 20% above actual field values showed an improvement of 5% of the cumulative production (an increase of 297 oil barrels), while the scenario in which wellhead pressure was 20% below showed a decrease of 11% of the cumulative production (a decrease of 483 oil barrels).

Pore pressures on day 34 for the three scenarios are presented in Figure 8, Figure 9 and Figure 10. The effect over the pressure gradient is evident. The higher pore pressure represents higher hydrocarbon content around the production zone.

The previously described models showed how the localized compaction process can be slowed down by controlling the production gradient. The pore pressure is less effective for expanding pores than confining pressure is for closing them; in consequence, choke management policy is crucial for hydrocarbon flow control and the delay of the subsequent compaction and loss of permeability.

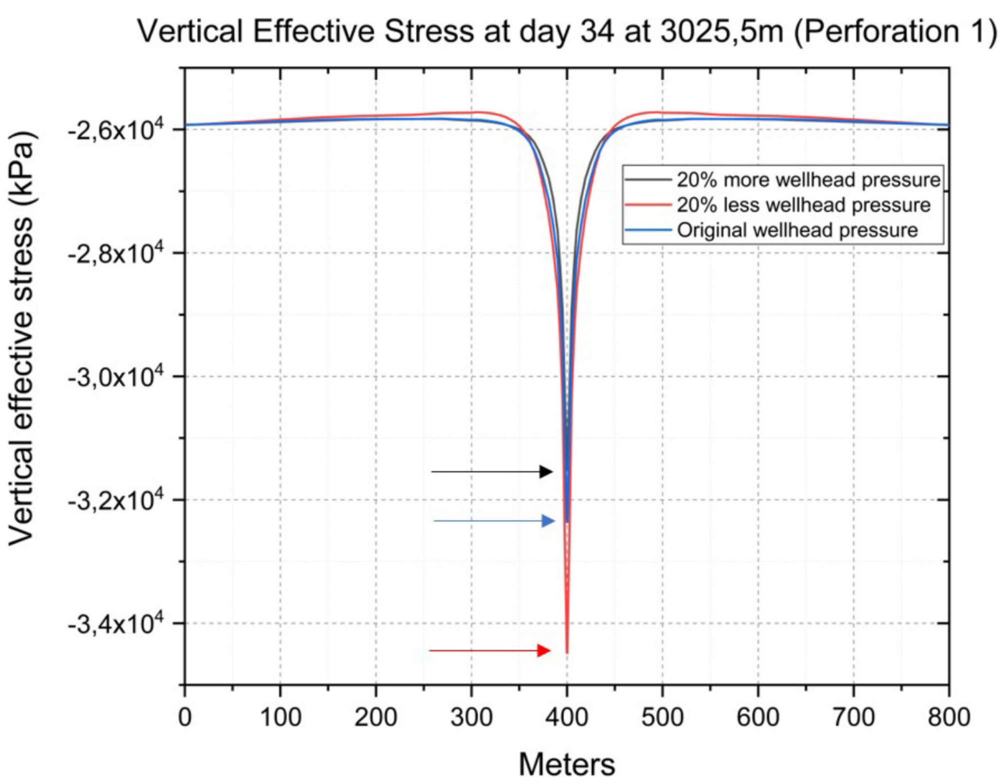

Figure 5. Effective vertical stress at Perforation 1 at different choke management scenarios.

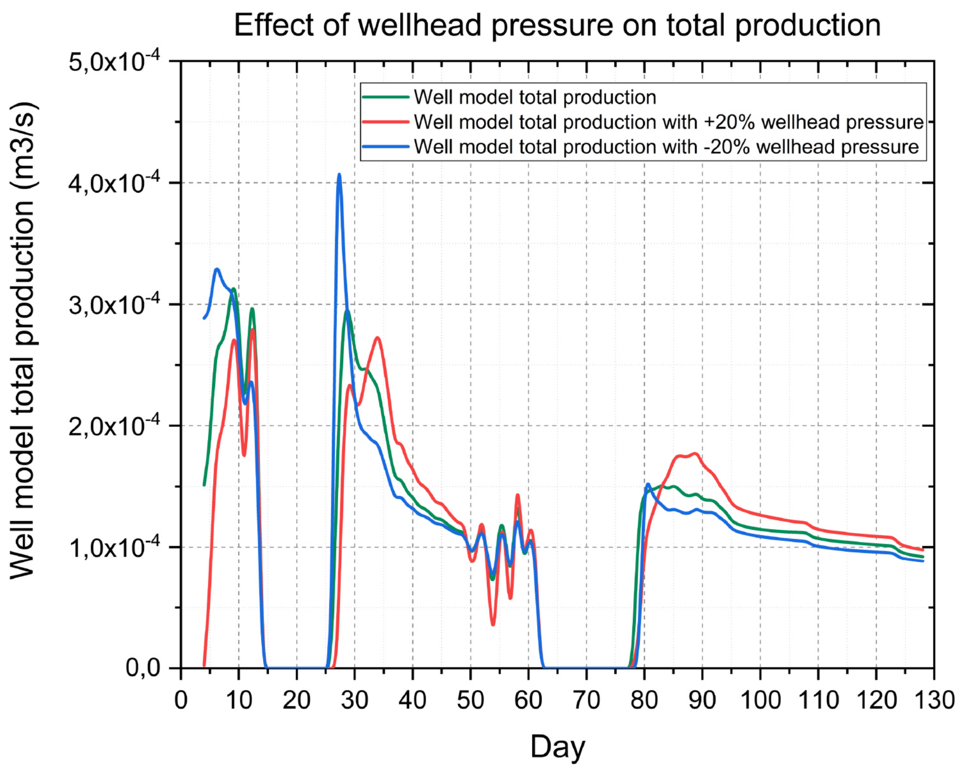

Figure 6. Production rates for different choke management scenarios.

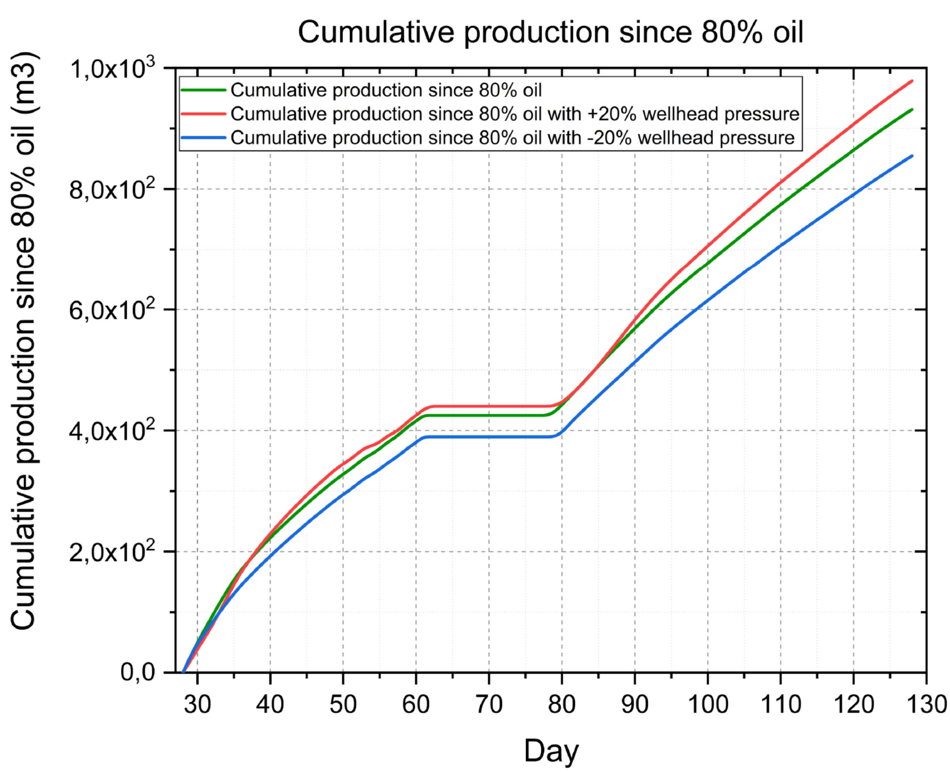

Figure 7. Cumulative production for different choke management scenarios.

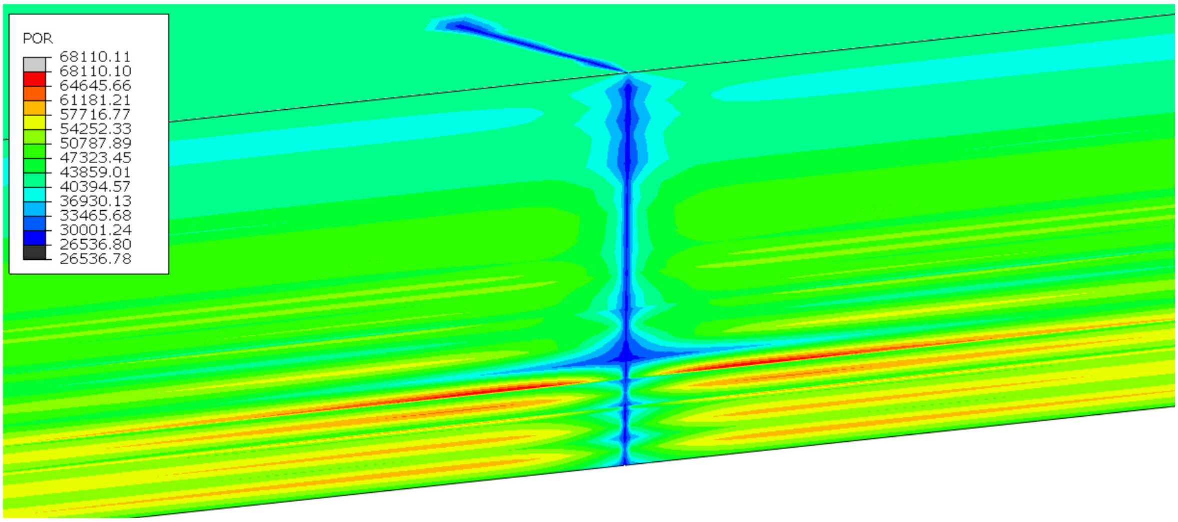

Figure 8. Pore pressure [KPa] on day 34 – field case choke management.

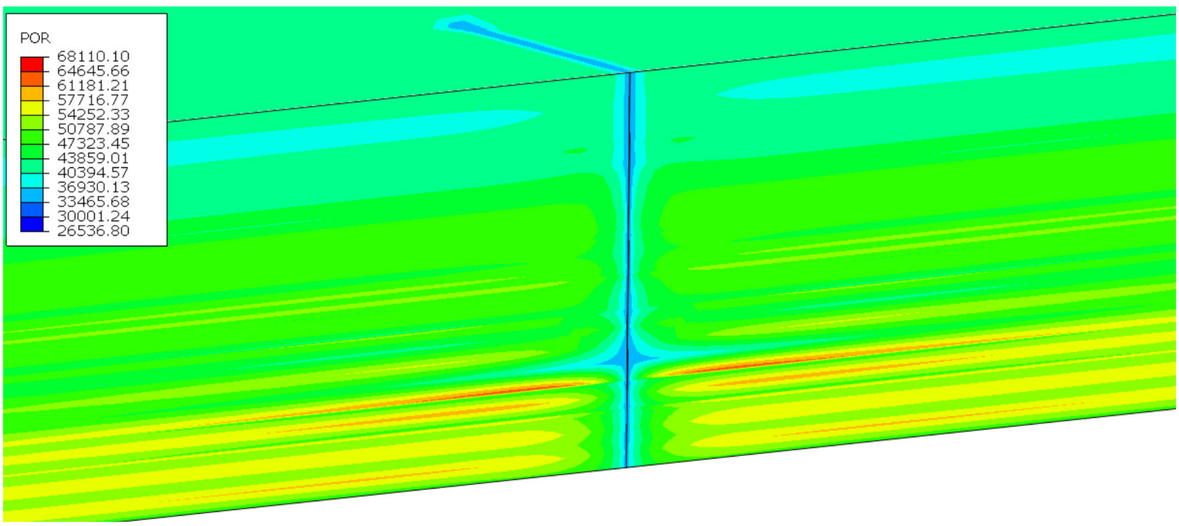

Figure 9. Pore pressure [KPa] on day 34. +20% wellhead pressure.

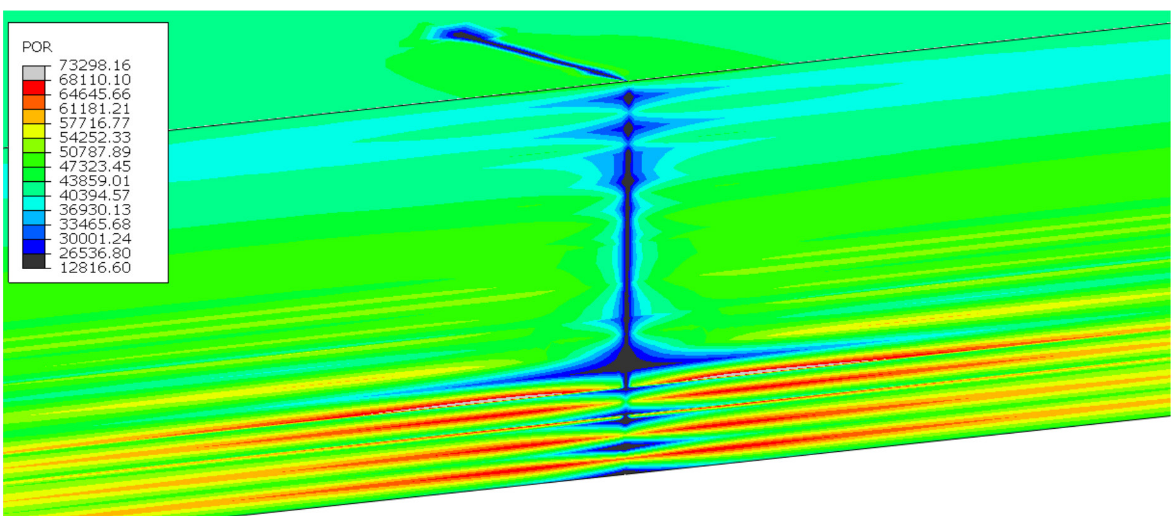

Figure 10. Pore pressure [KPa] on day 34. -20% wellhead pressure.

CONCLUSIONS

The present work demonstrates the advantages of having a comprehensive reservoir characterization and a 3D FEM porelastic geomechanical model when estimating hydrocarbon production from either vertical or horizontal wells. As shown in this paper, the FEM model allows predicting how the reservoir will evolve during its exploitation and, at the same time, allows an evaluation of the well integrity. The results obtained by means of the different numerical simulations show the impact that wellhead pressure management has on the reservoir permeability, and therefore on total hydrocarbon recovery. The scenario where wellhead pressure was 20% above actual field values showed an improvement of 5% of total oil recovery (increased by 297 oil barrels), while the scenario in which wellhead pressure was 20% below showed a decrease of 11% of total oil recovery (decreased by 483 oil barrels). The obtained results were based on a fixed increase/decrease of wellhead pressure of 20%, selected arbitrarily. The hydrocarbon recovery percentage may improve by choosing the optimal choke management scenario that maximizes hydrocarbon recovery and allows a faster return on investment.

APPENDIX

In order to calculate the pore pressure, the modified Eaton's equation using Vp(0º) was applied (Rezaee *et al.* 2015). For a porous, overpressured and low permeability VTI medium that behaves like a closed or open system under a normal stress regime, the wave velocity Vp (0º) will be the most sensitive to changes in effective stress and elastic symmetry of the rock (Vernik, 1994; Pinna *et al.* 2011; Carcione and Avseth 2015). The curve was calibrated with the DFIT measured in the Tordillo formation and is in agreement with the DFIT measured in a neighboring well within the VMF. The Sh and SH were calculated using the in-house algorithm to solve the poroelastic equation adopting the closure pressure as an upper boundary to adjust the Sh. In this case, as the zone was a critically stressed area of the crust, an approximation of Sh using the internal friction coefficient was used as lower boundary for the minimum stress (Zoback 2007). The resulting solution lies between these two limits. Breakouts found in other formations of the well were not used to estimate horizontal stress anisotropy since this ratio is strongly dependent on the Pp (Zoback 2007). In this case, the ratio between the Sh and the SH was obtained from numerical models using the caliper measurements (Fjaer *et al.* 2008).

Figure 11 shows the strain calculated by the algorithm. In green the minimum horizontal strain, in blue the maximum horizontal strain, and in red an average reference value usually used in the normal stress regime area are shown. The static elastic VTI tensor, along with the estimated Pp, Sv, strains, and Biots coefficients, resulted in the stress field shown in Figure 12.

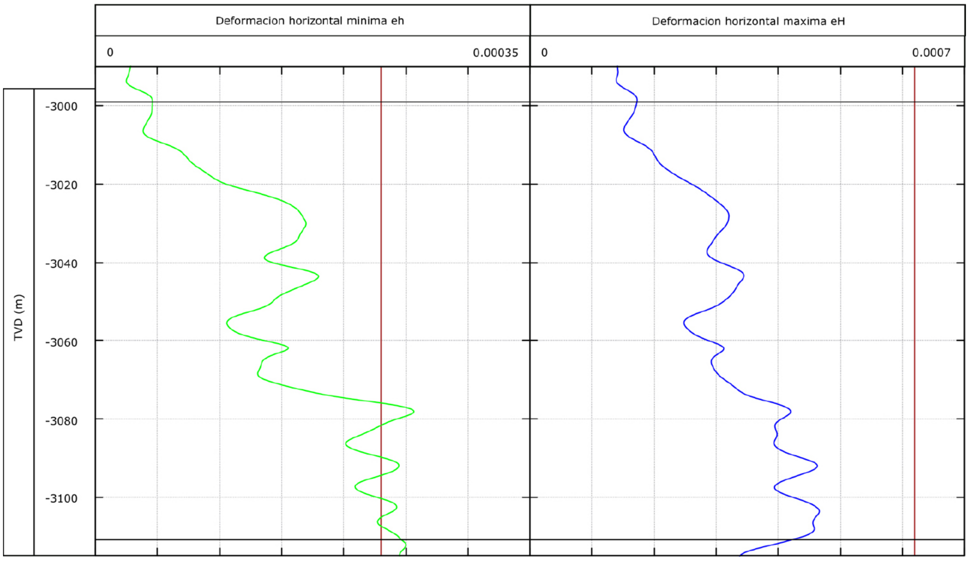

Figure 11. Horizontal strains.

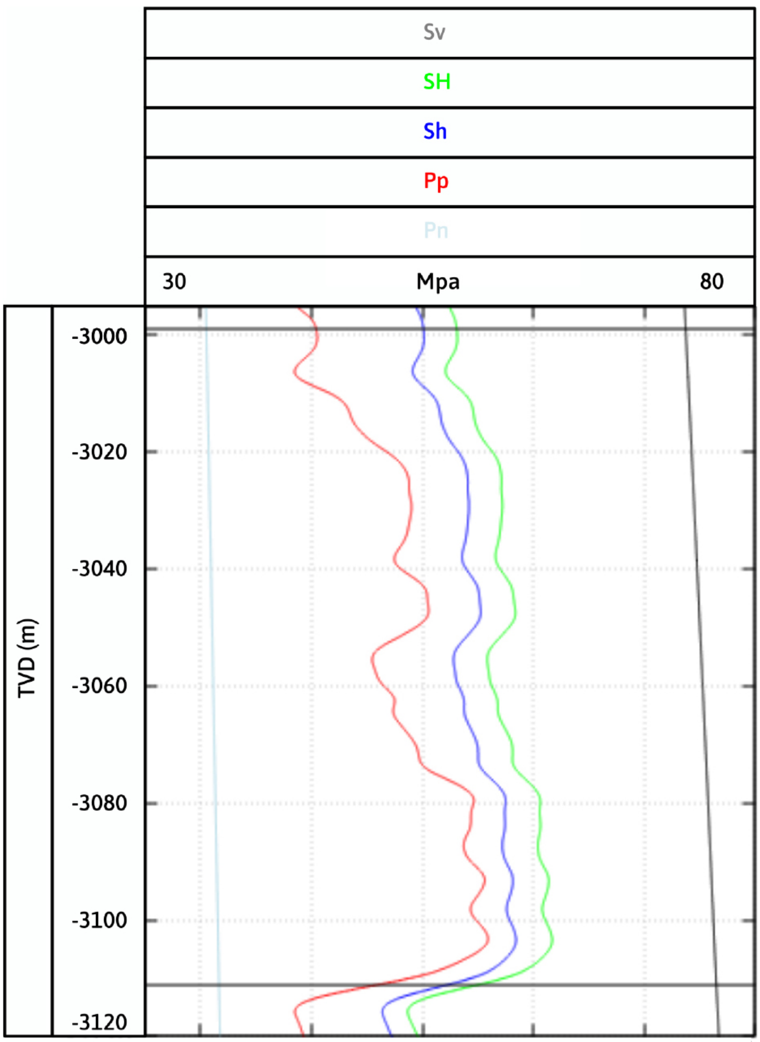

Figure 12. Stress field.

ACKNOWLEDGEMENTS

The authors would like to thank Tections S.A., Solaer Ingeniería S.A. and Pluspetrol S.A. for providing data and for authorizing the publication of this technical paper.

REFERENCES

Al Duhailan, M.A., Sonnenberg S.A, and Longman, M., 2015. Analyzing Beef Fractures: Genesis and Relationship with Organic-Rich Shale Facies. Paper presented at the SPE/AAPG/SEG Unconventional Resources Technology Conference, San Antonio, Texas, USA, doi: https://doi.org/10.15530/URTEC-2015-2151959.

Al Duhailan, M.A., Sonnenberg S.A, and Meckel L.D., 2013. Insights on Hydrocarbon-Generation Microfracturing in Organic-Rich Shales, Unconventional Resources Technology Conference, Denver, Colorado, USA.

Almasoodi, M., Vaidya, R., and Reza, Z., 2020. Drawdown-Management and Fracture-Spacing Optimization in the Meramec Formation: Numerical-and Economics-Based Approach. SPE Reservoir Evaluation & Engineering 23 (4): 1251-1264.

Apaydin, O.G., E. Ozkan, and R. Raghavan., 2012. Effect of Discontinuous Microfractures on Ultratight Matrix Permeability of a Dual-Porosity Medium. SPE Res Eval & Eng 15 (2012): 473–485. doi: https://doi.org/10.2118/147391-PA.

Arch, J., and Maltman, A., 1990. Anisotropic permeability and tormosity in deformed wet sediments structure in accrefionary tectonic features fluids flow from accrefionary within collement Project (DSDP)/ ODP drill holes which have penetrated major so the examination of microscopic s. Journal of Geophysical Research, 95(89), 9035–9045. https://doi.org/10.1029/JB095iB06p09035

Bagci, S., and Stolyarov, S., 2019. Flowback Production Optimization for Choke Size Management Strategies in Unconventional Wells. Paper SPE 196203, presented at the SPE Annual Technical Conference and Exhibition, Calgary, Alberta, Canada, 30 September-2 October.

Belyadi, H., E. Fathi, and F. Belyadi, 2019. Hydraulic Fracturing in Unconventional Reservoirs. Theories, Operations, and Economic Analysis. https://doi.org/10.1016/C2018-0-01643-6.

Bhandari, A.R., Flemings, P.B., Polito, P.J., Cronin, M.B., Bryant, S.L., 2015. Anisotropy and stress dependence of permeability in the Barnett shale. Transp. Porous Media 108 (2), 393e411.

Bryndzia, L.T and N.R. Braunsdorf., 2014. From Source Rock to Reservoir: The Evolution of Self-Sourced Unconventional Resource Plays. Elements 2014; 10 (4): 271–276. doi: https://doi.org/10.2113/gselements.10.4.271.

Carcione, J. M., and P. Avseth., 2015. Rock-physics templates for clay-rich source rocks. Geophysics, 80, no. 5, D481–D500, doi: 10.1190/GEO2014-0510.1.

Fjaer, E., R.Holt, P. Horsrud, A. Raaen, and R. Risnes., 2008. Petroleum Related Rock Mechanics, volume 53. Elsevier, 2nd ed.

Garcia, M.N., F. Sorenson, J.C Bonapace, F. Motta, C. Bajuk, and H. Stockman., 2013. Vaca Muerta Shale Reservoir Characterization and Description: The Starting Point for Development of a Shale Play with Very Good Possibilities for a Successful Project. URTeC paper 1508336 presented at the Unconventional Resources Technology Conference, Denver, Colorado, USA, 12-14 August 2013.

Gasparik, M., Bertier, P., Gensterblum, Y., Ghanizadeh, A., Krooss, B. M., & Littke, R., 2014. Geological controls on the methane storage capacity in organic-rich shales. International Journal of Coal Geology, 123, 34–51. https://doi.org/10.1016/j.coal.2013.06.010.

Ghanizadeh, A., A. Amann-Hildenbrand, M. Gasparik, Y. Gensterblum, B.M. Krooss, and R. Littke., 2013. Experimental study of fluid transport processes in the matrix system of the European organic-rich shales: II. Posidonia Shale. International Journal of Coal Geology, http://dx.doi.org/10.1016/j.coal.2013.06.009.

Hegazy, D.A., 2016. An experimental study to investigate the effects of in situ stress state and rock-fluid interactions on propped fracture conductivity in the Vaca Muerta formation. Master's thesis, Colorado School of Mines, Golden, Colorado.

Heller, R., Vermylen, J. P., & Zoback, M.D., 2014. Experimental investigation of matrix permeability of gas shales. AAPG Bulletin, 98(5), 975–995. https://doi.org/10.1306/09231313023

Hernández Bilbao, E., J. F. Sarg, and S. A. Sonnenberg., 2016. High-resolution chemostratigraphy, sequence stratigraphic correlation, porosity and fracture characterization of the Vaca Muerta Formation, Neuquén Basin, Argentina. Golden, Colorado, Colorado School of Mines.

Hryb, D.E., 2018. Efecto de la evolucion del Drawdown sobre la salud de la fractura hidráulica. ¿Podemos predecirlo?. 10th Congreso de Exploración y Desarrollo de Hidrocarburos, Simposio de Geomecánia, Mendoza, Argentina.

Iriarte, J., D. Hegazy, D. Katsuki, A.N. Tutuncu, Chapter 16., 2018. Fracture Conductivity Under Triaxial Stress Conditions, Editor(s): Yu-Shu Wu, Hydraulic Fracture Modeling, Gulf Professional Publishing, 2018, Pages 513-525, ISBN 9780128129982, https://doi.org/10.1016/B978-0-12-812998-2.00016-3.

Jagadisan, A. and Heidari, Z., 2019. Experimental Quantification of the Impact of Thermal Maturity of Kerogen on its Wettability. SPE Reservoir Evaluation & Engineering Journal, Formation Evaluation 22 (4): 1323 – 1333. DOI: 10.2118/195684-PA.

Karantinos, E., 2019. Choke Management and Production Optimization in Oil and Gas Fields Ph.D. Thesis. The University of Texas at Austin.

Lewan, M. D. and J. E. Birdwell., 2013. Application of Uniaxial Confining-core Clamp with Hydrous Pyrolysis in Petrophysical and Geochemical Studies of Source Rocks at Various Thermal Maturities. SPE/AAPG/SEG Unconventional Resources Technology Conference, Denver, Colorado, USA, August 2013. doi: https://doi.org/10.1190/urtec2013-267.

Lewan, M.D. and H. Allison., 1999. Gas:Oil Ratios for Source Rocks Containing Type-I, -II, -IIS, and -III Kerogens as Determined by Hydrous Pyrolysis. U.S. Geological Survey.

Lewan, M.D., 1985. Evaluation of petroleum generation by hydrous pyrolysis experimentation. Philosophical Transactions of the Royal Society of London, Series A 315, 123–134.

Lewan, M.D., and Roy,S., 2011. Role of water in hydrocarbon generation from Type-I kerogen in Mahogany oil shale of the Green River Formation. Elseiver, Organic Geochemistry 42 (2011) 31–41.

Lewan, M.D., and T.E Ruble., 2002. Comparison of petroleum generation kinetics by isothermal hydrous and nonisothermal open-system pyrolysis. Org. Geochem. 33, 1457–1475.

Loucks, R.G. and R.M. Reed., 2014. Scanning-Electron-Microscope Petrographic Evidence for Distinguishing Organic-Matter Pores Associated with Depositacional Organic Matter versus Migrated Organic Matter in Mudrocks. GCAGS Journal, v. 3, p. 5160.

Loucks, R.G., R.M. Reed, S.C. Ruppel, and U. Hammes., 2012. Spectrum of pore types and networks in mudrocks and a descriptive classification for matrix-related mudrock pores: American Association of Petroleum Geologists Bulletin, v. 96, p. 1071–1098, doi: 10.1306/08171111061.

Ma, X., and Zoback, M.D., 2017. Laboratory experiments simulating poroelastic stress changes associated with depletion and injection in low-porosity sedimentary rocks. Journal of Geophysical Research: Solid Earth, 122(4), 1–26. https://doi.org/10.1002/2016JB013668.

Mokhtari, M., Alqahtani, A. A., Tutuncu, A. N., & Yin, X., 2013. Stress-Dependent Permeability Anisotropy and Wettability of Shale Resources. In Unconventional Resources Technology Conference (pp. 2713–2728).

Mokhtari, M., and A.N. Tutuncu., 2015. Characterization of anisotropy in the permeability of organic-rich shales. Journal of Petroleum Science and Engineering, Volume 133, 2015, Pages 496-506, ISSN 0920-4105, https://doi.org/10.1016/j.petrol.2015.05.024.

Nelson, P.H., 2009. Pore-throat sizes in sandstones, tight sandstones, and shales. AAPG Bulletin 2009; 93 (3): 329–340. doi: https://doi.org/10.1306/10240808059.

Pan, Z., Y. Ma, L.D Connell, D.I Down, and M. Camilleri., 2015. Measuring anisotropic permeability using a cubic shale sample in a triaxial cell. Journal of Natural Gas Science and Engineering, Volume 26, Pages 336-344, ISSN 1875-5100, https://doi.org/10.1016/j.jngse.2015.05.036.

Pinna, G., J. M. Carcione, and F. Poletto., 2011. Kerogen to oil conversion in source rocks: Pore-pressure build-up and effects on seismic velocities. Journal of Applied Geophysics, 74, 229–235, doi: 10.1016/j.jappgeo.2011.05.006.

Ramos, R. and A. Sánchez Camus., 2017. Borehole cement sheath integrity-Numerical simulation under reservoir conditions. ENIEF, Mecánica Computacional Vol XXXV, págs. 193-225. La Plata, 7-10 noviembre.

Rezaee R., 2015. Fundamentals of Shale Gas Reservoir. Department of Petroleum Engineering Curtin University.

Rodrigues N., Cobbold P. R., Loseth H., and Ruffet G., 2009 Widespread bedding-parallel veins of fibrous calcite (beef) in a mature source rock (Vaca Muerta Fm, Neuquen Basin, Argentina): evidence for overpressure and horizontal compression. Journal of the Geological Society, 166(4):695709.

Ross, D. J. K. and Bustin, M., 2009. The importance of shale composition and pore structure upon gas storage potential of shale gas reservoirs. Marine and Petroleum Geology, 26(6), 916–927. https://doi.org/10.1016/j.marpetgeo.2008.06.004.

Saif, T., Lin, Q., Bijeljic, B., and Martin J.B, 2017. Microstructural imaging and characterization of oil shale before and after pyrolysis, Fuel, Volume 197, 2017, Pages 562-574, ISSN 0016-2361, https://doi.org/10.1016/j.fuel.2017.02.030.

Sánchez Camus, A. A., Ramos, R., and C. Rotili., 2021. Integral Characterization of the Vaca Muerta Formation. 3D Numerical Modeling of the Complete Cycle of a Vertical Well Located in the Oil Generation Window. Paper presented at the 55th U.S. Rock Mechanics/Geomechanics Symposium, Virtual, June 2021.

Sánchez Camus, A., P. Gauzellino, R. Ramos, and J.E Santos., 2018. Mudrock fractures characterization from well logs. AVO and AVAz analysis of the Quintuco-Vaca Muerta system and the Vaca Muerta-Tordillo system in the oil maturity window. 10th Congreso de Exploración y Desarrollo de Hidrocarburos, Simposio de Geofísica, Mendoza, Argentina, 2018: pp. 133–151.

Sosa Massaro, A., 2019. Estudio Geomecánico Regional de la Formación Vaca Muerta y su Aplicación a los Reservorios No Convencionales del tipo Shale oil/gas. Tesis doctoral, ITBA.

Ukar, E., R. G. López, D. Hryb, J. F. W. Gale, R. Manceda, A. Fall, I. Brisson, E. Hernandez-Bilbao, R. J. Weger, D. A. Marchal, A. Zanella, and P. R. Cobbold., 2020. Natural Fractures: From Core and utcrop Observations to Subsurface Models. Integrated Geology of unconventionals: The Case of the Vaca Muerta Play, Argentina. AAPG Memoir 121, 2020.

Vandenbroucke, M. and C. Largeau., 2007. Kerogen origin, evolution and structure. Organic Geochemistry, Volume 38, Issue 5, 2007, Pages 719-833, ISSN 0146-6380, https://doi.org/10.1016/j.orggeochem.2007.01. 001.

Varela, R.A., D. Marchal, S. Cuervo, E.F. Lombardo, Y.S. Perl, D.E. Hryb, P. Pateti, and O. Nielsen., 2020. Geomechanics: Pressure, stress field, and hydraulic fractures, in Daniel Minisini, Manuel Fantín, Iván Lanusse Noguera, and Héctor Leanza, eds., Integrated geology of unconventionals: The case of the Vaca Muerta play, Argentina: AAPG Memoir 121, p. 351–376.

Vernik, L. and X. Liu., 1997. Velocity anisotropy in shales: A petrophysical study. Geophysics, 62, no. 2, 521–532, doi: 10.1190/1.1444162.

Vernik, L., 1994. Hydrocarbon-generation-induced microcracking of source rocks. GEOPHYSICS, v. 59, no. 4, pp. 555-563.

Vernik, L., and A. Nur., 1992. Ultrasonic velocity and anisotropy of hydrocarbon source rocks. Geophysics, 57, 727–735, doi: 10.1190/1.1443286.

Vernik, L., and C. Landis, 1996 Elastic anisotropy of source rocks: Implications for hydrocarbon generation and primary migration. AAPG Bulletin, 80, 531–544.

Wan, J., R.S. Barnum, D.C. DiGloria, A. Leahy-Dios, R. Missman, and J. Hemphill., 2013. Factors Controlling Recovery in Liquids Rich Unconventional Systems. IPTC 17103, Beijing, China, 26–28.

Zee Ma, Y., and Holditch, S.A., 2016. Unconventional Oil and Gas Resources Handbook. Evaluation and Development. DOI: https://doi.org/10.1016/C2014-0-01377-9.

Zhao, Yajie, Yang, Hongzhi, Wu, Jianfa, Chang, Cheng, Liu, Chuxi, Yu, Wei, Li, Ning, and Kamy Sepehrnoori., 2021. "Choke Management Optimization for Shale Gas Reservoirs With EDFM."

Paper presented at the 55th U.S. Rock Mechanics/Geomechanics Symposium, Virtual, June 2021.

Zhou, J., L. Zhang, X. Li, and Z. Pan., 2019. Experimental and modeling study of the stress-dependent permeability of a single fracture in shale under high effective stress. Fuel, Volume 257, 2019, 116078, ISSN 0016-2361, https://doi.org/10.1016/j.fuel.2019.116078.

Zoback, M., 2007. Reservoir Geomechanics. Cambridge University Press

Zoback, M., and Kohli, A., 2019. Unconventional Reservoir Geomechanics: Shale Gas, Tight Oil, and Induced Seismicity. 10.1017/9781316091869.